Plasma Science and Technology

PAPER

Influence of target temperature on femtosecond laser-ablated brass plasma spectroscopy

To cite this article: Junfeng SHAO *et al* 2020 *Plasma Sci. Technol.* **22** 074001

Plasma Sci. Technol. **22** (2020) 074001 (7pp) https://doi.org/10.1088/2058-6272/ab7901

Influence of target temperature on femtosecond laser-ablated brass plasma spectroscopy

Junfeng SHAO (邵俊峰)[1], **Jin GUO** (郭劲)[1], **Qiuyun WANG** (王秋云)[2,3], **Anmin CHEN** (陈安民)[2,3,4] **and Mingxing JIN** (金明星)[2,3,4]

[1] State Key Laboratory of Laser Interaction with Matter & Innovation Laboratory of Electro-Optical Countermeasures Technology, Changchun Institute of Optics, Fine Mechanics and Physics, Chinese Academy of Sciences, Changchun 130033, People's Republic of China
[2] Institute of Atomic and Molecular Physics, Jilin University, Changchun 130012, People's Republic of China
[3] Jilin Provincial Key Laboratory of Applied Atomic and Molecular Spectroscopy (Jilin University), Changchun 130012, People's Republic of China

E-mail: amchen@jlu.edu.cn and mxjin@jlu.edu.cn

Received 22 November 2019, revised 20 February 2020
Accepted for publication 22 February 2020
Published 13 March 2020

Abstract

Spectral intensity, electron temperature and density of laser-induced plasma (LIP) are important parameters for affecting sensitivity of laser-induced breakdown spectroscopy (LIBS). Increasing target temperature is an easy and feasible method to improve the sensitivity. In this paper, a brass target in a temperature range from 25 °C to 200 °C was ablated to generate the LIP using femtosecond pulse. Time-resolved spectral emission of the femtosecond LIBS was measured under different target temperatures. The results showed that, compared with the experimental condition of 25 °C, the spectral intensity of the femtosecond LIP was enhanced with more temperature target. In addition, the electron temperature and density were calculated by Boltzmann equation and Stark broadening, indicating that the changes in the electron temperature and density of femtosecond LIP with the increase of the target temperature were different from each other. By increasing the target temperature, the electron temperature increased while the electron density decreased. Therefore, in femtosecond LIBS, a high-temperature and low-density plasma with high emission can be generated by increasing the target temperature. The increase in the target temperature can improve the resolution and sensitivity of femtosecond LIBS.

Keywords: laser-induced breakdown spectroscopy, time-resolved spectroscopy, emission enhancement, femtosecond laser, target temperature

(Some figures may appear in colour only in the online journal)

1. Introduction

Traditional spectral analysis methods include scanning electron microscopy, Raman spectroscopy, atomic absorption spectrometry, near-infrared spectroscopy, and atomic emission spectrometry (AES). As one of AES, laser-induced breakdown spectroscopy (LIBS) has a good application prospect in the field of element analysis. LIBS technique has many advantages such as fast and remote application [1–6], nearly nondestructive and *in situ* detection [7], and simplicity of design for field utilization [8, 9]. Its application field is very broad in material composition detection, such as soil composition detection, environmental governance, archeology, marine science, biomedicine [10–12]. Although LIBS technique has unique advantages and good application prospects, some bottlenecks gradually appear and hinder the

[4] Authors to whom any correspondence should be addressed.

development of LIBS detection technique. It is mainly manifested in the following three aspects: (1) lack of ability to detect molecular structure; (2) relatively low detection sensitivity and measurement accuracy; (3) matrix effect has a significant influence on detected results. In order to make up for the low detection sensitivity of LIBS technique, researchers have carried out a large number of studies on emission enhancement. Thus, many methods to enhance spectral emission are proposed, including spark assisted LIBS [13–16], spatial confined LIBS [17–21], double-pulse LIBS [22–28] and magnetic field confined LIBS [29–32], nanoparticle enhanced LIBS [33, 34], surface enhanced LIBS [35, 36], and preheated sample LIBS [37].

It is a simple and easy method to enhance emission line of LIP by preheating target. Eschlböck-Fuchs *et al* investigated the influence of the preheated target on the plume expansion and emission line of LIP, their results suggested that the higher temperature, the larger the volume of plume, the higher the brightness of plasma emission, and the stronger the intensity of spectral emission [38]. Tavassoli and Khalaji used a Nd:YAG laser to study the effect of preheated target on laser-ablated copper plasma, their results showed that the preheated target increased the spectral line emission by nearly 90%, but the initial target temperature has no effect on the background emission of LIP, which can effectively improve the signal-to-background ratio [39]. Hai *et al* investigated the effect of target temperature on the spectral line of laser-ablated molybdenum-tungsten plasma [40], their experiment was performed in a temperature range from 20 °C to 410 °C. Tavassoli and Gragossian studied the effect of the preheated target on the line intensity of LIBS, their results showed that the limit of detection was reduced by 40% when the sample was heated to 150 °C [41]. Zhang *et al* studied the effect of lens focusing distance on plume expansion of laser-ablated Si plasma under different target temperatures [42]. All of the above examples used nanosecond laser pulses to investigate the effect of sample temperature on spectral characteristics of LIP, while few researchers used femtosecond lasers to study the effect of sample temperature on the emission intensity.

Femtosecond laser relative to nanosecond laser has many outstanding characteristics, such as extremely narrow pulse width which can neglect plasma shielding effect, achieving faster continuous decay, and no delay detection. It can also increase the spectral emission and corresponding signal-to-background ratio, and it is easier to obtain a discrete spectrum, allowing a large number of spectra to be accumulated [43–49]. Since femtosecond laser has a very short pulse width, it is in a 'cold ablation' state. Therefore, increasing the temperature of the sample is interesting in studying the spectral characteristics of femtosecond LIP. In addition, due to the Stark effect [50], line broadening is used to determine electron density of LIP. When the electron density is high, the line broadening tends to widen, resulting in a decrease in the spectral resolution, thereby reducing the accuracy of element detection. To enhance spectral line resolution and intensity in LIBS, researchers are studying high-temperature and low-density plasma generation methods. He *et al* used re-excitation of laser-ablated particle to obtain high spectral resolutions by producing high-temperature and low-density plasmas [27]. Xu *et al* obtained high-temperature and low-density plasma produced by femtosecond laser by changing the focusing distance [51].

The spectral properties of LIBS are accompanied by dynamic decay process. Time-resolved spectroscopy can increase data information and enhance the understanding of various physical processes. In this paper, the time-resolved spectral emission of femtosecond laser-ablated brass at different target temperature was measured. Also, electron temperature and density were calculated based on Boltzmann plot and Stark broadening, and the time-resolved spectra presented the high-temperature and low-density characteristics of femtosecond LIP with higher sample temperature.

2. Experimental setup

The experimental setup for studying femtosecond laser-ablated brass plasmas under different target temperatures is displayed in figure 1. Femtosecond laser system used was a regeneration amplified Ti:sapphire laser (Libra, Coherent). The laser wavelength was 800 nm, and the pulse duration was 50 fs. The laser energy was adjusted by combining a half-wave plate with a Glan laser polarizer. A lens with a focal length of 100 mm was used to focus the pulse laser to target surface. The produced plasma emission was collected using two 75 mm focal length lenses with 50 mm diameter, and the collected light was transferred to a spectrometer (Spectra Pro 500i, PI Acton, 1200 grooves mm^{-1}). The optical signal was detected using an intensified charge-coupled device (ICCD, PI-MAX4, Princeton Instruments). In addition, the target was attached on the surface of a heating table by thermal grease compound. A thermocouple was used to monitor the temperature, and an electric heating resistor was used to heat the sample. When the target temperature increased, the thermocouple monitored the temperature and sent feedback to the heating resistor. If the temperature increased to a desired value, the heating resistor stopped heating; the temperature dropped, the heating resistor continued to heat the target. The heating table was used to increase the sample temperature and keep the sample temperature stable to ensure the stability of experimental data. The stability of the temperature is lower than 1 °C. The heating table was moved using a three-dimensional stage (PT3/Z8, Thorlabs) perpendicular to the laser. Each emission spectrum was an average of 100 pulses. The experimental measurement was performed in the atmosphere.

3. Results and discussion

In order to describe the change in the plasma emission under different sample temperatures, three clear copper spectral lines were selected, they were Cu(I) 510.55 nm ($3d^{10}4p^1(^2P_{3/2}) \rightarrow 3d^94s^2(^2D_{5/2})$), Cu(I) 515.32 nm ($3d^{10}4d^1(^2D_{3/2}) \rightarrow 3d^{10}4p^1(^2P_{1/2})$) and Cu(I) 521.82 nm

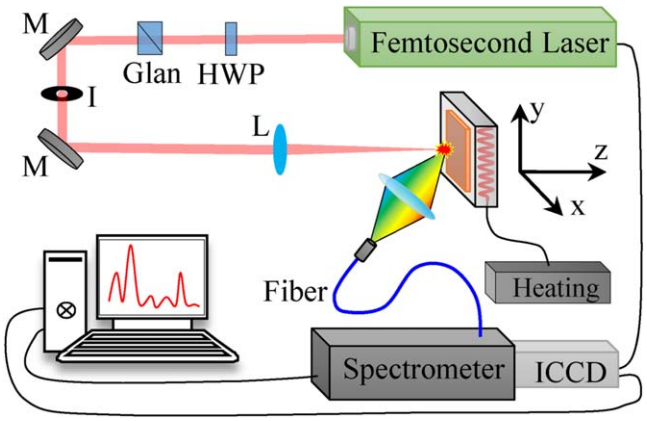

Figure 1. Experimental setup of femtosecond laser-induced pre-heated brass plasmas (HWP is the half-wave plate; Glan is the Glan laser polarizer; M is the mirror; I is the iris; L is the lens).

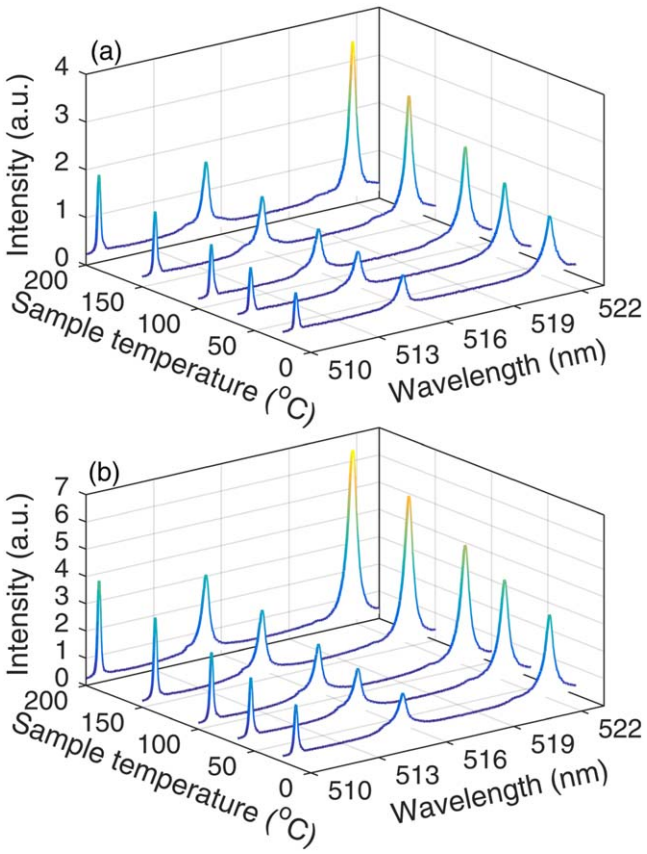

Figure 2. Typical emission spectra at different temperatures for 0.3 mJ (a) and 0.5 mJ (b) laser energies. Gate delay and width are 0.2 μs and 0.1 μs, respectively.

$(3d^{10}4d^{1}(^{2}D_{3/2}) \rightarrow 3d^{10}4p^{1}(^{2}P_{3/2}))$. Figure 2 presents the measured spectral distribution at sample temperatures of 25 °C, 65 °C, 100 °C, 150 °C and 200 °C in the wavelength range from 510 to 522 nm. As shown in figure 2, the emission line of laser-induced Cu plasma changes with a change in the sample temperature for 0.3 and 0.5 mJ laser energies. The intensities of three spectral lines show a monotonous increasing trend as the sample is heated from 25 °C to 200 °C.

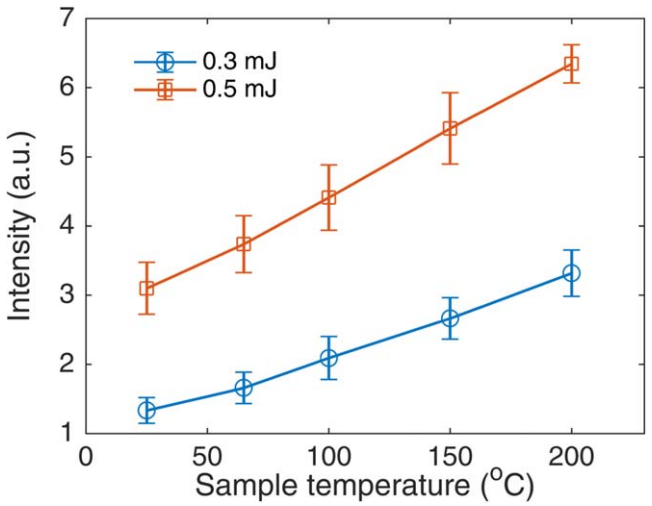

Figure 3. Evolutions of line peaks for Cu (I) 521.82 nm line with brass target temperature for 0.3 and 0.5 mJ laser energies. Gate delay and width are 0.2 and 0.1 μs.

Meanwhile, the background emission hardly changes with the increase of the brass temperature, improving signal-to-background ratio. The effect of preheated target and pulse energy on the line emission of LIBS is very important. To further analyze the influence of the preheated target and pulse energy on the emission line of brass plasma, the emission line at Cu (I) 521.8 nm with the target temperature is presented in figure 3.

As shown in figure 3, the peak of Cu (I) line at 521.82 nm increases with the increase of the target temperature for 0.3 mJ and 0.5 mJ laser energies. This phenomenon is caused by the following reasons:

(a) Reflectivity of metal

Under local thermal equilibrium (LTE), emission intensity of an atomic characteristic line can be described by the following formula [52]:

$$I_{\mathrm{k}} = C_{\mathrm{i}} M_{\mathrm{v}} \frac{A_{\mathrm{k}} g_{\mathrm{k}} hc}{Z\lambda_{\mathrm{k}}} \mathrm{e}^{-E_{\mathrm{k}}/kT_{\mathrm{e}}}, \tag{1}$$

where C_{i} is the element concentration in LIP, M_{v} is the amount of evaporated material in LIP (total mass of ablation), k is the Boltzmann constant, g_{k} is the degeneracy of spectral level (the statistical weight), and A_{k} represents the probability of spontaneous transition, h is the Planck constant, c is the light speed, Z is the partition function, λ_{k} is the emission wavelength, E_{k} is the upper level energy, and T_{e} is the electron temperature in plasma.

Equation (1) indicates that spectral intensity of plasma emission is mainly determined by the total mass of ablation M_{v}, and the electron temperature in plasma T_{e} [48]. The total ablation mass and the elemental density of the sample material determine the particle number in plasma. Because the electron temperature inside the plasma is very high (on the order of 10^4 K), the change in the target temperature causes little change in the line intensity of the LIP. For a fixed target to be tested, the relevant physical parameters in equation (1) are fixed values (can be found from NIST database), and they do not change as the sample temperature changes.

It can be seen that the intensity of the spectral emission is mainly affected by the maximum ablation mass M_v. This parameter can also characterize the maximum actual ablation efficiency produced by the coupling of pulsed laser energy and matter, calculated by the following formula [53]:

$$M_v = \frac{E_c}{C_p(T_b - T) + L}, \tag{2}$$

where T is the target temperature, L is latent heat, T_b is the evaporation temperature of the sample, C_p is the specific heat capacity.

$$E_c = E(1 - R(T)) \tag{3}$$

E_c is the coupling energy of pulsed laser and sample surface, E is the energy of the pulsed laser, and $R(T)$ is the reflectivity of the material surface. Equation (3) shows that, for fixed pulsed laser energy, the actual coupling energy E_c of the pulsed laser and the sample surface will increase due to the reduced reflectivity of the material surface, or decrease due to the increased reflectivity of the material surface, and has a certain inverse proportional linear relationship. At the same time, as the reflectivity of the sample surface is constant, the actual coupling energy E_c of the pulsed laser and the sample surface is proportional to the pulsed laser energy E.

It can be seen from equation (2) that the main factors affecting the maximum ablation mass M_v are the target temperature T, and the reflectivity $R(T)$ of the sample surface. The relationship between the surface reflectivity and the target temperature can be described as [54]:

$$R(T) = R_0 - R_1(T - T_0), \tag{4}$$

where R_0 is the reflectivity of the material surface at normal temperature T_0, R_1 is the coefficient determined by the properties of the material, and T is the temperature of the material. It is clear that the material reflectivity decreases with an increase in the material temperature.

According to the above physical mechanism, as the material temperature increased, the actual coupling energy of the laser pulse to the target surface increased, the total mass of the ablated sample increased, and the spectral intensity increased.

(b) Ablation threshold

As the sample was heated, the ablation threshold of the material decreased, and more material was ablated from target surface, resulting in an increase in the original internal energy of the brass target. Therefore, the plasma will gain more temperature [55].

(c) Air density

As the surface temperature of the brass target increased, the air near the brass surface was also heated, resulting in a decrease in the air density near the surface of the sample. This reduced the collision of particles in the air and the plasma, thereby reducing energy loss and increasing the spectral intensity of the plasma [38, 56, 57].

The generation and decay of LIBS are a dynamic process, thus the emission of the LIP changes over entire delay [56]. To better know the decay process of the LIP, we measured time-resolved spectra at different target temperatures. Figure 4 displays the time-resolved spectra at 25 °C and 200 °C target temperatures for 0.3 mJ laser energy. It is observed from the figure that the dynamic decay process of the three spectra is in the range of the delay time from 0 to 1.5 μs. After laser pulse, the LIP begins to cool, and the electron temperature begins to decrease. The optical emission of three spectral lines is dependent on the delay time. The spectral line under the condition of the preheated target (200 °C) is stronger than that under the condition of 25 °C. Increasing the target temperature can reduce the reflectivity and ablation threshold of the brass target. The preheated target can absorb more pulse energy, so the line intensity of the LIP is higher compared with low sample temperature. Therefore, the preheated target is equivalent to increasing the laser energy. In order to know the effect of the preheated target on the time-resolved spectroscopy, we selected the Cu (I) 521.82 nm to investigate the time-resolved emission peak intensities at different sample temperatures for 0.3 and 0.5 mJ laser energies.

The evolutions of Cu (I) 521.82 nm peak intensities with delay time at different sample temperatures for 0.3 and 0.5 mJ laser energies are presented in figure 5. The peak intensity first increases and then drops as the delay time increases. In the range of delay time from 0 to 0.2 μs, the spectral peak intensity increases, and reaches a maximum at 0.2 μs. As the delay time is longer than 0.2 μs, the peak intensity decreases monotonously. Moreover, the plasma emission duration of Cu (I) at 0.3 mJ laser energy is shorter than that at 0.5 mJ laser energy, that is, the plasma lifetime at low energy was lower than that at high energy. At the high laser energy, a stronger plasma can be produced and more particles in the plasma are excited [58]. In addition, the peak intensity is enhanced as the target temperature increases. When the temperature of the preheated target rises from 25 °C to 200 °C, the maximum enhancement factor of the spectral peak intensity is about 2.6 for 0.3 mJ laser energy. The spectral line at 0.3 mJ and 200 °C is stronger than that at 0.5 mJ and 25 °C. This indicates that the preheated brass target is equivalent to an increase in the laser energy. Therefore, increasing the target temperature plays an important role in enhancing the spectral intensity.

High-intensity laser pulsed radiation sample will produce high-temperature and high-density plasmas [59]. The plasmas with higher temperature can improve the sensitivity of LIBS, while the plasmas with higher density will reduce spectral resolution. This is because high-density plasmas increase line broadening due to the Stark effect (electrons in the plasma generate electric fields and can disturb the energy levels of the ions, causing the spectral lines of these high-energy levels to be broadened) [50]. Since line resolution in LIBS is critical to identify the spectra and determine the elements, it is important to generate the high-temperature and low-density plasmas. Next, we investigated the changes in electron temperature and density as the temperature of the target increased.

The electron density and temperature of the LIP are important physical parameters in LIBS. They can help us understand the kinetic processes in the plasma. The electron temperature of the LIP can be obtained by using measured intensity of spectral line. Under the LTE, the electron

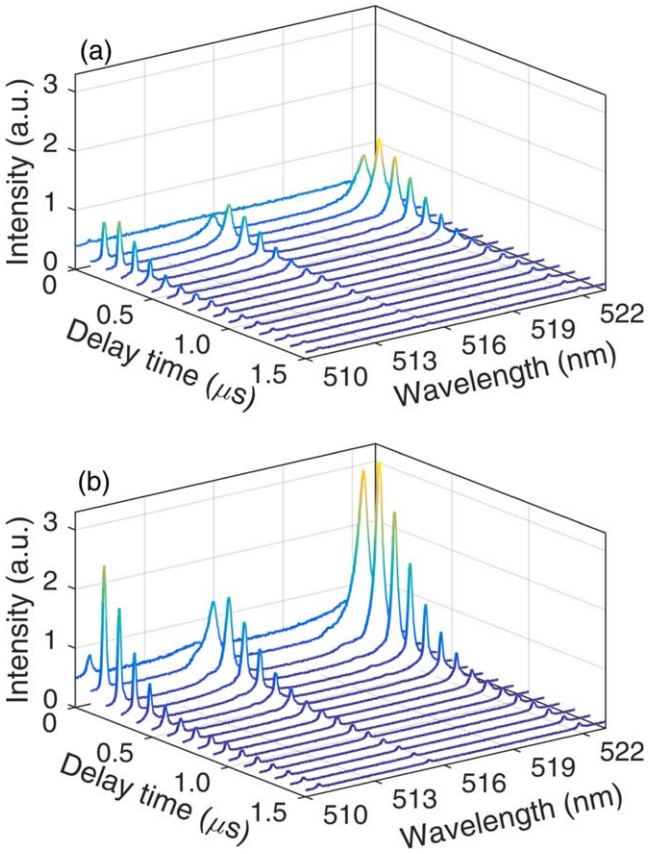

Figure 4. Time-resolved spectra for 25 °C (a) and 200 °C (b) target temperatures at 0.3 mJ laser energy.

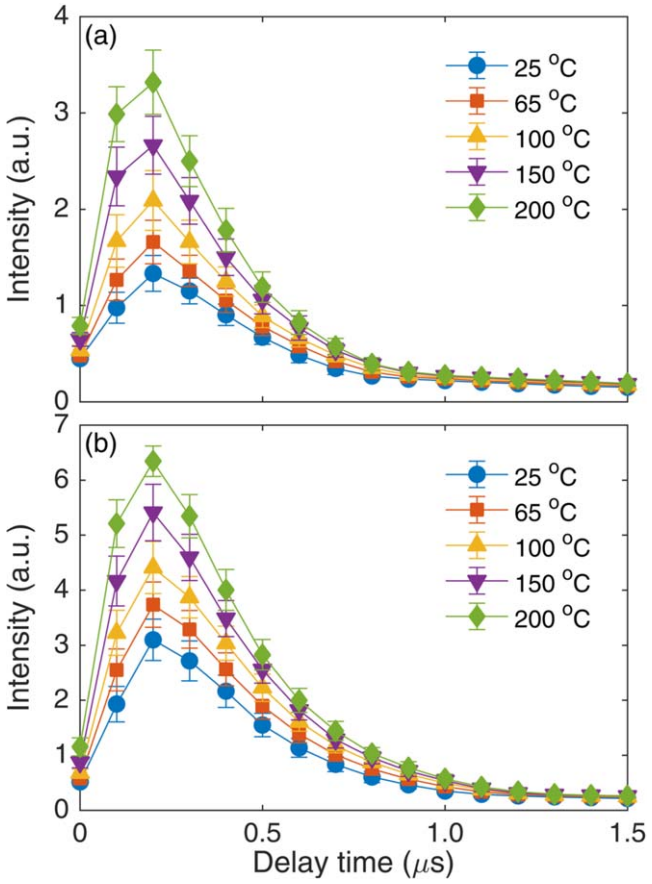

Figure 5. Evolutions of Cu (I) 521.82 nm peak intensities with delay time at different target temperatures for 0.3 mJ (a) and 0.5 mJ (b) laser energies.

temperature is calculated by Boltzmann plot [60, 61]:

$$\ln\left(\frac{\lambda_k I_k}{g_k A_k}\right) = -\frac{E_k}{kT_e} + C. \tag{5}$$

The parameters in equation (5) are listed in table 1 [62]. The temperature is calculated by the slope $(-1/kT_e)$ of the term $(\ln(\lambda_k I_k/g_k A_k))$ versus the upper energy (E_k). Many investigators selected Cu (I) lines at 510.55, 515.32 and 521.82 nm to obtain the Boltzmann plot [32, 34, 63]. In the current study, these three lines also were used to calculate the electron temperature.

Figure 6 presents the evolutions of electron temperatures with the delay time at 25 °C, 65 °C, 10 °C, 150 °C, and 200 °C target temperatures for 0.3 and 0.5 mJ laser energies. The electron temperature decreases with the increase of the delay time, and the temperature at low energy is lower than that at high energy. At fixed laser energy, the electron temperature increases with the increase of the brass temperature. The preheated target compared with the condition of 25 °C can make the ejected plasma obtain higher temperature, the number of particles in the upper energy level of Cu plasma increases, and the electron temperature of the plasma increases. The preheated condition can lower the ablation threshold of Cu sample, and more mass is ablated under the same pulse energy. In other words, the density of the plasma ejected will increase, resulting in a stronger collision within the particle, so the electron temperature of the plasma will increase.

Table 1. Physical parameters of Cu (I) lines [62].

Wavelength (nm)	E_k (eV)	g_k	A_{ki} (10^8 s^{-1})
510.55	3.82	4	0.02
515.32	6.19	4	0.60
521.82	6.19	6	0.75

The stark broadening effect is a common method for obtaining electron density. The contribution to the spectral line broadening mainly comes from electron broadening and ion broadening, while the ion broadening as compared to the electron impact is very small and can be ignored. Therefore, the full width at half maximum has the following relationship with the electron density n_e due to the spectral Stark broadening [64–66]:

$$\Delta\lambda_{1/2} = 2\omega\left(\frac{n_e}{10^{16}}\right). \tag{6}$$

The electron collision coefficient ω can be found in the [67]. The Cu (I) 521.82 nm was used to calculate the electron density. Since the electron density of the plasma is very large in the early stage of plasma expansion, the Stark broadening effect dominates the broadening of the spectral line. Meanwhile, the spectral line broadening also includes instrument

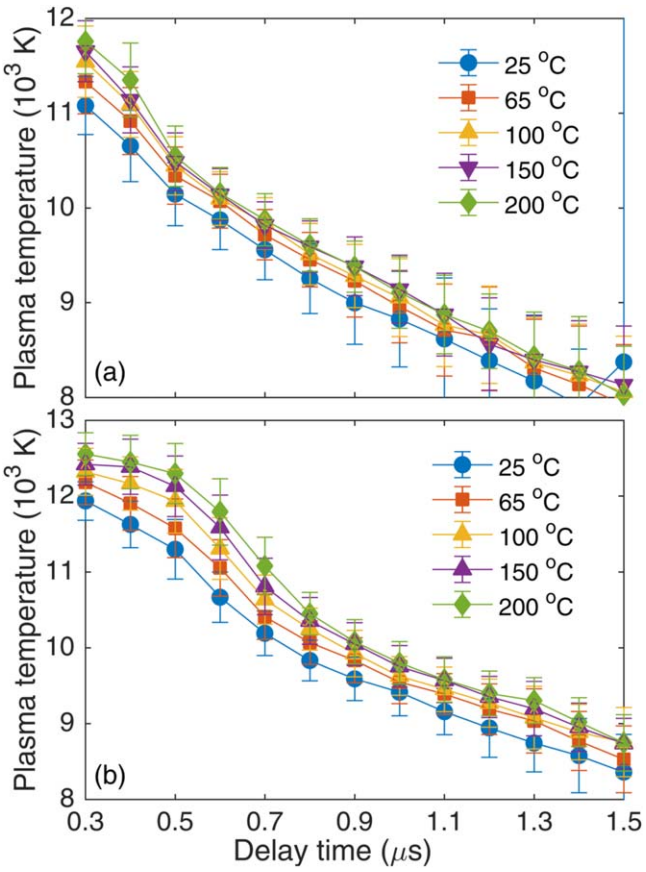

Figure 6. Evolutions of electron temperatures with the delay time at different target temperatures for 0.3 (a) and 0.5 mJ (b) laser energies.

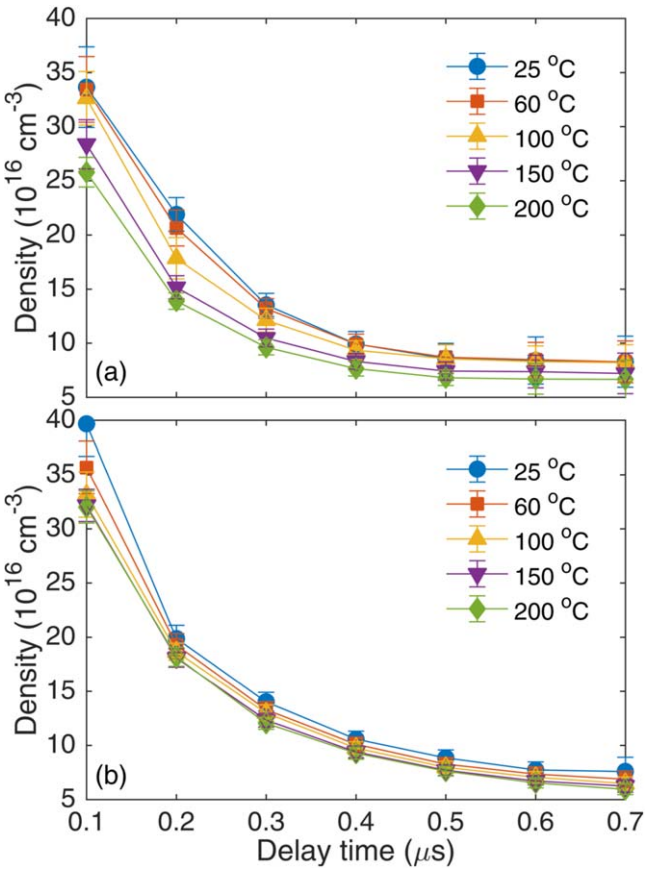

Figure 7. Evolutions of electron densities with the delay time at different target temperatures. Laser energies are 0.3 mJ (a) and 0.5 mJ (b).

broadening ($\Delta\lambda_{\text{inst}}$), Doppler broadening, and natural broadening. The Doppler broadening and natural broadening can be ignored. The instrument broadening approximated 0.04 nm, as determined by measuring the width of the Hg lines emitted by a mercury spectral lamp at low pressure. The measured line width ($\Delta\lambda_{\text{meas}}$) can be corrected by $\Delta\lambda_{1/2} = \Delta\lambda_{\text{meas}} - \Delta\lambda_{\text{inst}}$.

Figure 7 presents the evolutions of electron densities with the delay time at different brass target temperatures for 0.3 and 0.5 mJ laser energies. The electron density decreases with increasing the delay time. The femtosecond pulse ablates the target and rapidly generates plasma on the surface, resulting in the maximum electron density of the plasma. As the delay time increases, the plasma plume expands rapidly and the electron density decreases. In addition, different from the electron temperature, as the temperature of the sample increases, the electron density decreases. Since the experiment was carried out in air, the preheating not only heats the sample but also heats the air around the sample. According to the Clapeyron equation, air density is inversely proportional to temperature in an atmospheric environment [68]. When the sample temperature increases from 25 °C to 200 °C, the air density near the sample surface at 200 °C (473 K) became approximately 0.63 times at 25 °C (approximately 298 K). The density of the air around the sample decreases, and the plasma plume expands more dramatically, so the electron density decreases as the brass target is heated. Therefore, by means of preheating the sample, a high-temperature and low-density plasma with a strong spectral intensity in femtosecond LIBS can be obtained, thereby increasing the spectral resolution and the detection sensitivity.

4. Conclusion

We used femtosecond pulse laser to excite brass to study the effect of the preheated target on the spectral properties of the LIP. It was found that the preheated experimental condition can increase the spectral emission intensity of femtosecond laser-ablated brass plasma, and the time-resolved spectroscopy can better demonstrate the dynamic process of spectral decay in LIBS. We obtained time-resolved spectral intensities, electron temperatures and densities at different brass target temperatures. The obtained time-resolved spectral intensities and electron temperatures increased as the temperature of the sample increased, while the electron density decreased. Therefore, the preheating treatment of the target can obtain a strong emission, high-temperature and low-density plasma, thereby improving the spectral line resolution and the sensitivity of LIBS. We think that the study contributed to the development of femtosecond LIBS in scientific research and application.

Acknowledgments

We acknowledge the support by National Natural Science Foundation of China (Nos. 11674128, 11674124 and 11974138) and the Jilin Province Scientific and Technological Development Program, China (No. 20170101063JC).

References

[1] Hahn D W and Lunden M M 2000 *Aerosol Sci. Technol.* **33** 30
[2] Wang Z, Dong F Z and Zhou W D 2015 *Plasma Sci. Technol.* **17** 617
[3] Wang Z *et al* 2014 *Front. Phys.* **9** 419
[4] Wang Z Z *et al* 2016 *Front. Phys.* **11** 114213
[5] Wang Q Q *et al* 2012 *Front. Phys.* **7** 701
[6] Fu Y Y *et al* 2019 *Plasma Sci. Technol.* **21** 030101
[7] Nicolas G, Mateo M P and Piñon V 2007 *J. Anal. At. Spectrom.* **22** 1244
[8] Winefordner J D *et al* 2004 *J. Anal. At. Spectrom.* **19** 1061
[9] Barbini R *et al* 2002 *Spectrochim. Acta* B **57** 1203
[10] Haider A F M Y and Khan Z H 2012 *Opt. Laser Technol.* **44** 1654
[11] Sancey L *et al* 2016 *Sci. Rep.* **6** 24377
[12] Harilal S S *et al* 2018 *Appl. Phys. Rev.* **5** 021301
[13] Zhou W D *et al* 2013 *J. Anal. At. Spectrom.* **28** 702
[14] Zhou W D *et al* 2010 *Opt. Express* **18** 2573
[15] Kexue L I *et al* 2010 *Spectrochim. Acta* B **65** 420
[16] Wang Q Y *et al* 2019 *Plasma Sci. Technol.* **21** 065504
[17] Shen X K *et al* 2007 *Appl. Phys. Lett.* **91** 081501
[18] Wang Q Y *et al* 2018 *Phys. Plasmas* **25** 073301
[19] Shen X K *et al* 2007 *J. Appl. Phys.* **102** 093301
[20] Guo L B *et al* 2011 *Opt. Express* **19** 14067
[21] Wang Y *et al* 2016 *J. Anal. At. Spectrom.* **31** 1974
[22] Rashid B *et al* 2011 *Phys. Plasmas* **18** 073301
[23] Shen J *et al* 2015 *Plasma Sci. Technol.* **17** 147
[24] Sun D X *et al* 2014 *Plasma Sci. Technol.* **16** 374
[25] Lin X M, Li H and Yao Q H 2015 *Plasma Sci. Technol.* **17** 953
[26] Wang Y *et al* 2019 *Plasma Sci. Technol.* **21** 034013
[27] He X N *et al* 2011 *Opt. Express* **19** 10997
[28] Chen A M *et al* 2015 *Opt. Express* **23** 24648
[29] Harilal S S *et al* 2005 *IEEE Trans. Plasma Sci.* **33** 474
[30] Lu Y *et al* 2015 *J. Anal. At. Spectrom.* **30** 2303
[31] Pandey P K and Thareja R K 2013 *Phys. Plasmas* **20** 022117
[32] Singh K S and Sharma A K 2016 *Phys. Plasmas* **23** 122104
[33] De Giacomo A *et al* 2013 *Anal. Chem.* **85** 10180
[34] Chen A M *et al* 2015 *Phys. Plasmas* **22** 033301
[35] Aguirre M A *et al* 2013 *Spectrochim. Acta* B **79–80** 88
[36] Yang X Y *et al* 2017 *Talanta* **163** 127
[37] Darbani S M R *et al* 2014 *J. Eur. Opt. Soc.: Rapid Publ.* **9** 14058
[38] Eschlböck-Fuchs S *et al* 2013 *Spectrochim. Acta* B **87** 36
[39] Tavassoli S H and Khalaji M 2008 *J. Appl. Phys.* **103** 083118
[40] Hai R *et al* 2019 *J. Anal. At. Spectrom.* **34** 2378
[41] Tavassoli S H and Gragossian A 2009 *Opt. Laser Technol.* **41** 481
[42] Zhang D *et al* 2020 *Optik* **202** 163511
[43] Li S C *et al* 2015 *Appl. Surf. Sci.* **355** 681
[44] Wang T F *et al* 2015 *Phys. Plasmas* **22** 033106
[45] Wang X W *et al* 2018 *J. Anal. At. Spectrom.* **33** 168
[46] Chen A M *et al* 2011 *Opt. Commun.* **284** 2192
[47] Guo J *et al* 2012 *Opt. Commun.* **285** 1895
[48] Zhang D *et al* 2017 *Opt. Laser Technol.* **96** 117
[49] Wang Q Y *et al* 2020 *Opt. Laser Technol.* **122** 105862
[50] Pandey P K, Gupta S L and Thareja R K 2015 *Phys. Plasmas* **22** 073301
[51] Xu W P *et al* 2019 *J. Anal. At. Spectrom.* **34** 1018
[52] Sabsabi M and Cielo P 1995 *Appl. Spectrosc.* **49** 499
[53] Kuzuya M *et al* 1993 *Appl. Spectrosc.* **47** 1659
[54] Cristoforetti G *et al* 2004 *Spectrochim. Acta* B **59** 1907
[55] Ujihara K 1972 *J. Appl. Phys.* **43** 2376
[56] Guo K M *et al* 2019 *AIP Adv.* **9** 065214
[57] Harilal S S *et al* 2012 *Phys. Plasmas* **19** 083504
[58] LaHaye N L *et al* 2014 *J. Appl. Phys.* **115** 163301
[59] Shaikh N M *et al* 2013 *Spectrochim. Acta* B **88** 198
[60] Wang Y *et al* 2018 *Phys. Plasmas* **25** 033302
[61] Yang D P *et al* 2017 *Acta Phys. Sin.* **66** 115201
[62] Wang Y *et al* 2020 *Phys. Plasmas* **27** 023507
[63] Zorba V, Mao X L and Russo R E 2015 *Spectrochim. Acta* B **113** 37
[64] Bashir S *et al* 2012 *Appl. Phys.* **107** 203
[65] Wang Y *et al* 2020 *Opt. Laser Technol.* **122** 105887
[66] Wang Q Y *et al* 2019 *J. Anal. At. Spectrom.* **34** 1242
[67] Hafez M A *et al* 2003 *Plasma Sources Sci. Technol.* **12** 185
[68] Zhang D *et al* 2018 *Phys. Plasmas* **25** 083305